Recursive evaluation of interaction forces of unbounded soil in time domain

M.Motosaka
*Kobori Research Complex, Kajima Corporation, Tokyo, Japan**
J.P.Wolf
Electrowatt Engineering Services Ltd, Zürich, Switzerland

1. INTRODUCTION

To be able to analyze soil-structure interaction in the time domain, the contribution of the unbounded soil to the basic equation of motion of the structure-soil system (Fig. 1) is specified in the form of convolution integrals (Wolf, 1988) as

$$\{R_{r,b}(t)\} = \int_0^t [S^g_{r,bb}(t-\tau)](\{u^t_b(\tau)\} - \{u^g_b(\tau)\})d\tau \qquad (1)$$

$\{R_{r,b}(t)\}$ denotes the regular part of the interaction forces acting at the nodes b located on the structure-soil interface (P_b, R_b in the two-dimensional case illustrated in Fig. 1), $[S^g_{r,bb}(t)]$ the regular part of the dynamic-stiffness coefficients of the unbounded soil (system ground g) in the time domain, $\{u^t_b(t)\}$ and $\{u^g_b(t)\}$ the total and generalized scattered displacements, respectively. The subscripts b,r and the superscripts t and g are dropped for the sake of conciseness in the following.

As the boundary condition expressed in equation 1 is global in time, i.e. all degrees of freedom of the nodes on the structure-soil interface from the start of the excitation contribute to the forces, the computational effort is significant. To be able to reduce the latter, the convolution integrals in time are evaluated recursively at each time step. In this method, the interaction forces $\{R\}_n$ at time $t = n\Delta t$ are computed from the nth displacements $\{u\}_n$ and the M and L past values of the interaction forces and displacements, respectively. To evaluate a typical convolution integral appearing in equation 1, written as

$$\{R\}_n = \int_0^t [S(t-\tau)]\{u(\tau)\}\, d\tau \qquad (2)$$

the recursive formulation leads to

$$\{R\}_n = \sum_{i=1}^{M} [a]_i\{R\}_{n-i} + \Delta t \sum_{i=0}^{L} [b]_i\{u\}_{n-i} \qquad (3)$$

*presently at Electrowatt Engineering Services Ltd.

$[a]_i$ and $[b]_i$ are matrices of constants to be determined. The recursive evaluation, although in general only approximate, makes the analysis of soil-structure interaction in the time domain competitive with that performed in the frequency domain. The same concepts can also be used in a flexibility formulation. The storage requirements are also reduced.

Recursive formulations have hardly been used in the analysis of soil-structure interaction. A notable exception is described in Verbic 1973, which corresponds to the impulse-invariant way discussed in Section 2. Section 3 describes another possibility to derive a recursive relation based on a segment approach using z-transforms. An illustrative example is examined in Section 4, and in Section 5 the number of operations is addressed. This compact paper is based on Wolf and Motosaka 1988.

2. IMPULSE-INVARIANT METHOD

The M+L+1 unknown matrices $[a]_i$, $[b]_i$ in equation 3 are calculated by solving a system of equations which are established by equating the rigorous and recursive formulations for a discretized unit impulse displacement at the first M+L+1 time steps. Applying this unit-impulse displacement in the form of a triangle (zero at $t = 0$, increasing linearly up $t = \Delta t$ where the value equals $1/\Delta t$ and then decreasing linearly up to $t = 2\Delta t$) for all degrees of freedom denoted as $\{1/(\Delta t)\}$ and substituting into equation 2 lead to

$$\{R\}_n = [S]_{n-1} \{\frac{1}{\Delta t}\} \tag{4}$$

with

$$[S]_{n-1} = \int_0^{\Delta t} [S(n\Delta t-\tau)] \frac{\tau}{\Delta t} d\tau + \int_0^{\Delta t}[S((n-1)\Delta t-\tau)](1- \frac{\tau}{\Delta t}) d\tau \tag{5}$$

For n=1 ($t=\Delta t$) only the first term on the right-hand side of equation 5 arises. Equation 4 is formulated for the first M+L+1 steps and is equated to the recursive equation 3 which is applied repeatedly and substituted into equation 3. This results in the system of equations. For a general M and L applied to a multi-degree-of-freedom system, the equations are specified in Wolf and Motosaka 1988. for M=L=1, this procedure leads to

$$[a]_1 = [S]_1^{-1} [S]_2 \tag{6a}$$

$$[b]_o = \frac{1}{\Delta t} [S]_o \tag{6b}$$

$$[b]_1 = \frac{1}{\Delta t} ([S]_1 - [S]_1^{-1} [S]_2[S]_o) \tag{6c}$$

Assuming the dynamic-stiffness coefficient S(t) to be piecewise linear over each time step, the recursive formulation for M=L=1 and for a one-degree-of-freedom system leads to

$$R_n = \frac{S(\Delta t)+4S(2\Delta t)+S(3\Delta t)}{S(0) +4S(\Delta t) +S(2\Delta t)} R_{n-1} + \frac{2S(0) + S(\Delta t)}{6} u_n\Delta t$$
$$+ \frac{1}{6}[S(0)+4S(\Delta t)+S(2\Delta t)- \frac{S(\Delta t)+4S(2\Delta t)+S(3\Delta t)}{S(0) +4S(\Delta t) +S(2\Delta t)} (2S(0)+S(\Delta t))] u_{n-1}\Delta t \tag{7}$$

If the dynamic-stiffness coefficient in the frequency domain is a ratio of polynomials and if M and L-1 are selected equal to the degrees of the polynomials of the denominator and numerator, respectively, it can be shown that this recursive formulation leads to rigorous results. For a more general dynamic-stiffness coefficient, M and L should be chosen to be about equal. Increasing M (and L) leads to more accurate results, but the system of equations to be solved tends to become numerically singular. This tendancy is increased for smaller Δt. When the dynamic-stiffness coefficient in the time domain is calculated numerically by applying the FFT, zig-zagging of S(t) for small t can arise, as the high-frequency contribution has to be neglected. This can cause divergence of the solution for small M and L.

3. SEGMENT APPROACH BASED ON Z-TRANSFORM

For accurate results it is often necessary to represent a large range of the dynamic-stiffness coefficient S(t) for an arbitrary Δt, whereby the numerical singularity discussed above has to be avoided. In addition, it is desirable to determine the coefficient $[a]_i$, $[b]_i$ of the recursive equation 3 without solving a system of equations. Such an explicit formulation is especially important for the case of a system with many degrees of freedom. These two goals are met by the following method called the segment approach.

In the segment approach, the unit-impulse function S(t) is divided into segments. In each segment S(t) is approximated by the product of a polynomial and an exponential function with a negative exponent, of which the z-transform can be determined analytically. Selecting the same type of interpolation functions for all degrees of freedom and for all segments results in the same diagonal $[a]_i$-matrix which is equal to a scalar multiplied by the unit matrix. This property reduces further the computational effort. The $[b]_i$-matrix will, in general, be fully populated.

$[S(t)]$ is approximated using second-degree polynomials as follows (Fig. 2)($\bar{t}$ = dimensionless time).

$$[S(\bar{t})] = \sum_{i=1}^{N} ([c_o]_i+[c_1]_i\bar{t}+[c_2]_i\bar{t}^2)\exp(-\bar{t})(H(\bar{t}-\bar{t}_{i-1})-H(\bar{t}-\bar{t}_i)) \quad (8)$$

N is the number of segments, $[c_j]_i$ are the coefficients of the i-th segment (j=0,1,2) determined from the values at the beginning, center and end of each segment, $\bar{t}_i$ is the time at the end of the i-th segment and H is the Heaviside step function. Equation 8 is rewritten as

$$[S(\bar{t})] = \sum_{i=1}^{N} \exp(-\bar{t}_{i-1})([d_o]_i+[d_1]_i(\bar{t}-\bar{t}_{i-1})+[d_2]_i(\bar{t}-\bar{t}_{i-1})^2)$$
$$\cdot\exp[-(\bar{t}-\bar{t}_{i-1})](H(\bar{t}-\bar{t}_{i-1}))-([c_o]_N+[c_1]_N\bar{t}+[c_2]_N\bar{t}^2)\exp(-\bar{t})H(\bar{t}-\bar{t}_N) \quad (9)$$

with

$$[d_o]_i = [c_o]_i-[c_o]_{i-1}+([c_1]_i-[c_1]_{i-1})\bar{t}_{i-1}+([c_2]_i-[c_2]_{i-1})\bar{t}^2_{i-1}$$

$$[d_1]_i = [c_1]_i - [c_1]_{i-1} + 2([c_2]_i - [c_2]_{i-1})\bar{t}_{i-1}$$

$$[d_2]_i = [c_2]_i - [c_2]_{i-1} \tag{10}$$

The second term on the right-hand side of equation 9 is deleted, which adds an exponentially decaying tail to the approximation for $\bar{t} > \bar{t}_N$.

To derive the corresponding recursive equation for the total system corresponding to equation 9, it is sufficient to examine one element in one term of the sum. Applying the shifting theorem and deleting a constant term, the latter is formulated as

$$h(\bar{t}) = (d_o + d_1\bar{t} + d_2\bar{t}^2)\exp(-\bar{t}) \tag{11}$$

To be able to apply the z-transform, equation 11 is discretized with the values selected at the middle of the time step, resulting in

$$h(n) = (d_o + d_1(\frac{2n+1}{2})\Delta\bar{t} + d_2(\frac{2n+1}{2})^2\Delta\bar{t}^2)\exp(-\frac{2n+1}{2}\Delta\bar{t}) \quad n=0,1,.. \tag{12}$$

The z-transform equals

$$H(z) = \sum_{n=0}^{\infty} h(n)\, z^{-n} \tag{13}$$

which leads to

$$H(z) = \frac{(d_o + \frac{\Delta\bar{t}}{2}d_1 + \frac{\Delta\bar{t}^2}{4}d_2)\exp(-\frac{\Delta\bar{t}}{2}) + (-2d_o + \frac{3\Delta\bar{t}^2}{2}d_2)\exp(-\frac{3\Delta\bar{t}}{2})z^{-1} + (d_o - \frac{\Delta\bar{t}}{2}d_1 + \frac{\Delta\bar{t}^2}{4}d_2)\exp(-\frac{5\Delta\bar{t}}{2})z^{-2}}{1 - 3\exp(-\Delta\bar{t})z^{-1} + 3\exp(-2\Delta\bar{t})z^{-2} - \exp(-3\Delta\bar{t})z^{-3}} \tag{14}$$

Formulating the input-output relationship in the z-domain

$$P(z) = H(z)\, U(z) \tag{15}$$

and performing the inverse z-transform results in

$$\begin{aligned} P_n &= 3\exp(-\Delta\bar{t})\, P_{n-1} - 3\exp(-2\Delta\bar{t})\, P_{n-2} \\ &+ \exp(-3\Delta\bar{t})\, P_{n-3} + (d_o + \frac{\Delta\bar{t}}{2}d_1 + \frac{\Delta\bar{t}^2}{4}d_2)\exp(-\frac{\Delta\bar{t}}{2})\, U(n) \\ &+ (-2d_o + \frac{3\Delta\bar{t}^2}{2}d_2)\exp(-\frac{3\Delta\bar{t}}{2})\, U(n-1) \\ &+ (d_o - \frac{\Delta\bar{t}}{2}d_1 + \frac{\Delta\bar{t}^2}{4}d_2)\exp(-\frac{5\Delta\bar{t}}{2})\, U(n-2) \end{aligned} \tag{16}$$

Substituting

$$U(n) = \frac{\Delta\bar{t}}{2}(u_{n-1} + u_n) \tag{17}$$

leads to

$$P_n = 3\exp(-\Delta\bar{t})\, P_{n-1} - 3\exp(-2\Delta\bar{t})\, P_{n-2} + \exp(-3\Delta\bar{t})\, P_{n-3}$$
$$+ \left(\frac{d_o}{2} + \frac{\Delta\bar{t}}{4} d_1 + \frac{\Delta\bar{t}^2}{8} d_2\right) \exp\left(-\frac{\Delta\bar{t}}{2}\right) u_n \Delta\bar{t}$$
$$+ \left(\frac{d_o}{2} - d_o \exp(-\Delta\bar{t}) + \frac{\Delta\bar{t}}{4} d_1 + \frac{\Delta\bar{t}^2}{8} d_2 + \frac{3}{4}\Delta\bar{t}^2 d_2 \exp(-\Delta\bar{t})\right)\exp\left(-\frac{\Delta\bar{t}}{2}\right)u_{n-1}\Delta\bar{t}$$
$$+ \left(-d_o + \frac{d_o}{2}\exp(-\Delta\bar{t}) - \frac{\Delta\bar{t}}{4} d_1 \exp(-\Delta\bar{t}) + \frac{3}{4}\Delta\bar{t}^2 d_2\right.$$
$$\left. + \frac{\Delta\bar{t}^2}{8} d_2 \exp(-\Delta\bar{t})\right) \exp\left(-\frac{3\Delta\bar{t}}{2}\right) u_{n-2}\Delta\bar{t}$$
$$+ \left(\frac{d_o}{2} - \frac{\Delta\bar{t}}{4} d_1 + \frac{\Delta\bar{t}^2}{8} d_2\right) \exp\left(-\frac{5\Delta\bar{t}}{2}\right) u_{n-3}\Delta\bar{t} \qquad (18)$$

Returning to equation 9 and applying the shifting theorem results in the final recursive equation

$$\{R\}_n = 3\exp(-\Delta\bar{t})[I]\{R\}_{n-1} - 3\exp(-2\Delta\bar{t})[I]\{R\}_{n-2}$$
$$+ \exp(-3\Delta\bar{t})[I]\{R\}_{n-3} + \Delta\bar{t} \sum_{i=1}^{N} \exp(-\bar{t}_{i-1}) \sum_{j=0}^{3} [b_i]_j \{u\}_{n-j-n_{i-1}} \qquad (19)$$

where

$$[b_i]_0 = \left(\frac{[d_o]_i}{2} + \frac{\Delta\bar{t}}{4}[d_1]_i + \frac{\Delta\bar{t}^2}{8}[d_2]_i\right)\exp\left(-\frac{\Delta\bar{t}}{2}\right)$$
$$[b_i]_1 = \left(\frac{[d_o]_i}{2} - [d_o]_i \exp(-\Delta\bar{t}) + \frac{\Delta\bar{t}}{4}[d_1]_i + \frac{\Delta\bar{t}^2}{8}[d_2]_i\right.$$
$$\left. + \frac{3}{4}\Delta\bar{t}^2[d_2]_i \exp(-\Delta\bar{t})\right)\exp\left(-\frac{\Delta\bar{t}}{2}\right)$$
$$[b_i]_2 = \left(-[d_o]_i + \frac{[d_o]_i}{2}\exp(-\Delta\bar{t}) - \frac{\Delta\bar{t}}{4}[d_1]_i \exp(-\Delta\bar{t})\right.$$
$$\left. + \frac{3}{4}\Delta\bar{t}^2[d_2]_i + \frac{\Delta\bar{t}^2}{8}[d_2]_i \exp(-\Delta\bar{t})\right)\exp\left(-\frac{3\Delta\bar{t}}{2}\right)$$
$$[b_i]_3 = \left(\frac{[d_o]_i}{2} - \frac{\Delta\bar{t}}{4}[d_1]_i + \frac{\Delta\bar{t}^2}{8}[d_2]_i\right)\exp\left(-\frac{5\Delta\bar{t}}{2}\right) \qquad (20)$$

and with $n_{i-1} = \bar{t}_{i-1}/\Delta\bar{t}$.

4. SEMI-INFINITE ROD ON ELASTIC FOUNDATION

As an illustrative example the semi-infinite rod on an elastic foundation (Fig. 3) which exhibits the characteristic properties of the unbounded soil (Wolf 1986) is addressed. The undamped rod with area A, modulus of elasticity E, mass density ρ and spring coefficient per unit length k_g is subjected to a prescribed support movement at point 0.

$$u_o(\bar{t}) = \frac{u_o}{2}\left[1-\cos\left(2\pi \frac{\bar{t}}{\bar{t}_o}\right)\right], \quad 0 < \bar{t} < \bar{t}_o, \quad u_o(\bar{t}) = 0, \quad \bar{t} > \bar{t}_o \qquad (21)$$

The dimensionless time $\bar{t} = tc_l\kappa$ with $c_l = \sqrt{E/\rho}$ and $\kappa = \sqrt{k_g/(EA)}$ and $\bar{t}_o = 2$. The dimensionless reaction force $\bar{P}_o(\bar{t}) = P_o(\bar{t})/(K^g u_o)$ equals (Wolf 1986)

$$\bar{P}_o(\bar{t}) = \frac{d\bar{u}_o(\bar{t})}{d\bar{t}} + \int_o^{\bar{t}} \frac{1}{\bar{t}-\bar{\tau}} J_1(\bar{t}-\bar{\tau})\bar{u}_o(\bar{\tau})\, d\bar{\tau} \qquad (22)$$

with $\bar{u}_o(\bar{t}) = u_o(\bar{t})/u_o$ and $K = \sqrt{EAk_g}$. The second term on the right-hand side of equation 22 represents the regular part of the reaction force, consisting of a convolution integral of the regular part of the dynamic-stiffness coefficient $J_1(\bar{t})/\bar{t}$ and of the displacement $\bar{u}_o(\bar{t})$. $J_1(\bar{t})$ is the Bessel function of the first order and of the first kind. $\bar{P}_o(\bar{t})$ determined directly from equation 22 is plotted as a dashed line in the following figures.

Selecting a larger number for M and L in the impulse-invariant method improves the accuracy (Fig. 4). It is worth mentioning that already for M=L=4 and $\Delta\bar{t}$ = 0.1 a numerical singularity arises. A better agreement also occurs when for a fixed M=L=3 a larger $\Delta\bar{t}$ is used (Fig. 5). The result of the impulse-invariant method with M=L=3 is compared to that of the segment approach with only one segment and with $\bar{t}_1$ = 1.4 which leads to the same computational effort, in Fig. 6. As the segment approach adds a decaying tail for the range $\bar{t}$ > 1.4, the accuracy is superior to that of the impulse-invariant method. Both incorporate the dynamic-stiffness coefficient up to $\bar{t}$ = 1.4. As expected, increasing the number of segments improves the accuracy (Fig. 7).

5. NUMBER OF OPERATIONS

The number of operations in evaluating the convolution integrals in the various methods is determined as follows. N^t denotes the number of time steps, N^s the number of boundary elements introduced in the spatial discretization (with 3 degrees of freedom per element).

The direct evaluation of the convolution integral (equation 2) requires

$$\frac{(N^t)^2}{2} (3N^s)^2 \qquad (23)$$

operations. The impulse-invariant method (equation 3) leads to the following number of operations

$$N^t(M+L+1)\ (3N^s)^2 \qquad (24)$$

In the segment approach (equation 19), it is assumed that the number of time steps (=$t_1/\Delta t$) in each segment is the same. For this case, the number of operations is specified as

$$N^t 3(3N^s) + [N^t 4N - 2N(N-1)\ t_1/\Delta t]\ (3N^s)^2 \qquad (25)$$

As an example, an earthquake time history of 30s duration with a Δt = 0.005 s is addressed, resulting in N^t = 6000. For 20 three-dimensional boundary elements (N^s = 20) the number of operations for the three methods is compared in Table 1. For the segment approach N and $t_1/\Delta t$ are varied as indicated. For one segment, a dramatic reduction of almost three orders of magnitude occurs. The storage requirement (= $(t_{N-1}/\Delta t + 7)3N^s$) of the segment approach is reduced compared to that of the direct evaluation, but is larger than that of the impulse-invariant way (= $(M+L+1)3N^s$), which also leads to a significant reduction in the number of operations.

REFERENCES

Wolf J.P. 1988. Soil-Structure-Interaction Analysis in Time Domain. Englewood Cliffs, NJ: Prentice-Hall

Verbic B. 1973. Analysis of Certain Structure-Foundation Systems, Ph.D. dissertation, Department of Civil Engineering, Rice Univ., Houston, TX

Wolf J.P. and Motosaka M. 1988. Recursive Evaluation of Interaction Forces of Unbounded Soil in Time Domain, submitted for review and possible publication in Earthquake Engineering and Structural Dynamics

Wolf J.P. 1986. A Comparison of Time-Domain Transmitting Boundaries, Earthquake Engineering and Structural Dynamics, 14, 655-673

Table 1: Number of Operations for Evaluation of Convolution Integrals

Direct Evaluation	Impulse-Invariant Method M=L=3	Segment Approach				
		N \ $t_1/\Delta t$	60 $(0.01\ N^t)$	150 $(0.025\ N^t)$	300 $(0.05\ N^t)$	600 $(0.1\ N^t)$
$6.5 \cdot 10^{10}$	$1.5 \cdot 10^{8}$	1	$8.7 \cdot 10^{7}$	$8.7 \cdot 10^{7}$	$8.7 \cdot 10^{7}$	$8.7 \cdot 10^{7}$
		2	$1.73 \cdot 10^{8}$	$1.72 \cdot 10^{8}$	$1.70 \cdot 10^{8}$	$1.65 \cdot 10^{8}$
		3	$2.58 \cdot 10^{8}$	$2.54 \cdot 10^{8}$	$2.47 \cdot 10^{8}$	$2.34 \cdot 10^{8}$
		4	$3.42 \cdot 10^{8}$	$3.34 \cdot 10^{8}$	$3.21 \cdot 10^{8}$	$2.95 \cdot 10^{8}$

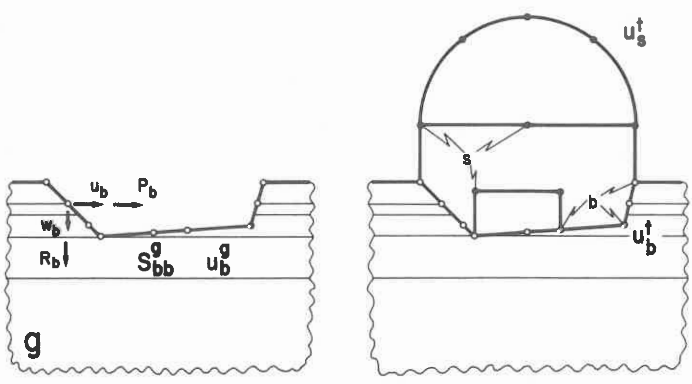

Fig. 1 Unbounded Soil and Structure-Soil System

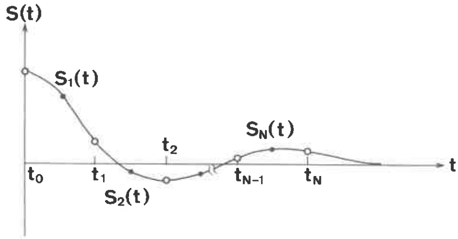

Fig. 2 Subdivision of Dynamic-Stiffness Coefficient into Segments

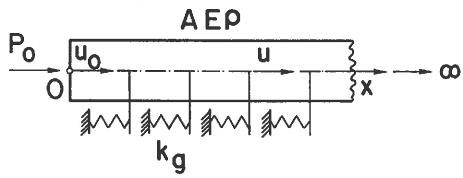

Fig. 3 Semi-Infinite Rod on Elastic Foundation

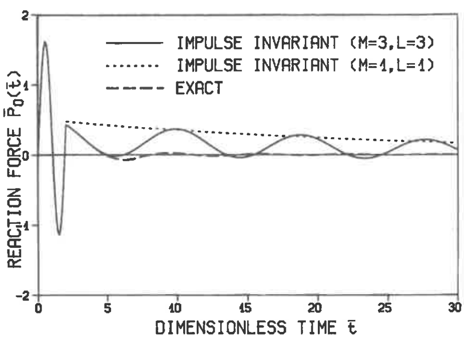

Fig. 4 Varying M and L of Impulse-Invariant Method ($\Delta\bar{t}$ = 0.1)

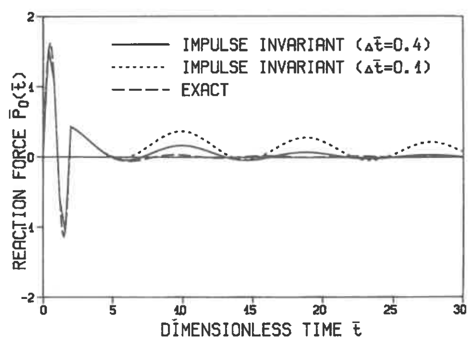

Fig. 5 Varying $\Delta\bar{t}$ of Impulse-Invariant Method (M=L=3)

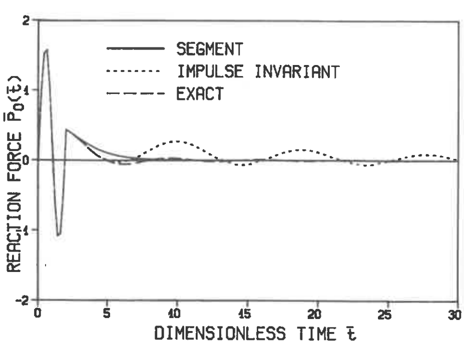

Fig. 6 Comparison of Segment Approach and Impulse-Invariant Method (Δt = 0.2)

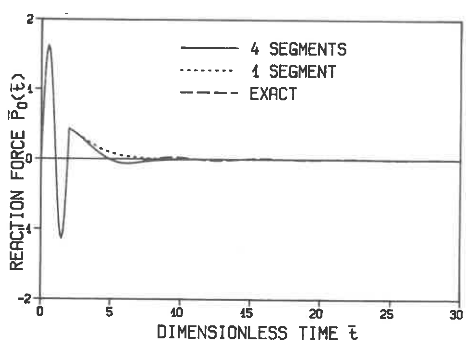

Fig. 7 Varying Number of Segments ($\Delta\bar{t}$ = 0.1)